Electronic Supplementary Information

Stable Bismuth Phosphosulfide Nanoparticles Encapsulated into Hollow Multi-Channel Carbon Nanofibers Toward High Performance Sodium Storage

*Linlin Li,[a] Hongcheng Jiang,[a] Na Xu,[a] Xintong Lian,[a] Hongjiao Huang,[a] Hongbo Geng,[*b] and Shengjie Peng*[a]*

[a]College of Materials Science and Technology, Nanjing University of Aeronautics and Astronautics, Nanjing 210016, China. E-mail: pengshengjie@nuaa.edu.cn

[b] School of Materials Engineering, Changshu Institute of Technology, Changshu, Jiangsu 215500, China. E-mail: genghonhbo@126.com

Experimental Section

Materials synthesis: (i) Preparation of Bi@MCNFs. First, 0.75 g $BiCl_3$ was dissolved into 8 mL DMF. Then 1 g polyacrylonitrile (PAN, Mw = 150,000) and 0.5 g polystyrene (PS, Mw = 192,000) were added into the above solution and stirred at 60 °C overnight. The obtained homogeneous precursor solution was used as the electrospun solution. The injection rate was accurately controlled to be 0.8 mL h^{-1}, and the voltage was adjusted to 20 kV. After electrospinning, the collected nanofibers were stabilized in the air at 280 °C for 2 hours and calcined in the reducing gas (Ar (95 vol %) / H_2 (5 vol %)) at 700 °C for 6 hours to obtain Bi@MCNFs nanofibers. (ii) Preparation of $BiPS_4$@MCNFs. The as-obtained Bi@MCNFs were ground in an agate mortar with red phosphorus and sulfur powder at a molar ratio of 1: 1: 4 and then transferred into a vacuum quartz tube. The sealed quartz tube was calcined in a muffle furnace at 600 °C with a heating rate of 5 °C min^{-1} for five days. $BiPS_4$@MCNFs were synthesized after the operation. (iii) Preparation of $BiPS_4$@CNFs and $BiPS_4$ bulk. $BiPS_4$@CNFs and $BiPS_4$ bulk were prepared with a similar process to $BiPS_4$@MCNFs, using the Bi@CNFs and commercial Bi powder as the Bi source. For $BiPS_4$@CNFs, no PS was used during the electrospinning process.

Structural and morphology characterizations: The phase composition was performed by an X-ray diffraction (XRD, Bruker D8 Advance) with Cu-Kα radiation (λ = 1.5418 Å). The elemental content was investigated by X-ray photoelectron spectrometry (XPS, Esca lab 250Xi, Thermo Fisher Scientific), corrected by the C 1s line at 284.8 eV. The thermogravimetric analysis (TGA, STA 449F3, NETZSCH) was to explore the distribution of the target materials. Raman microscope tested the carbon content (Raman spectra, Thermo Fischer DXR). The crystal morphology was demonstrated by scanning electron microscopy (SEM, Regulus 8100, Hitachi). Transmission

electron microscope (TEM, FEI Tecnai G2 F20, 15 kV) and high-resolution transmission electron microscopy (HRTEM) with energy-dispersive X-ray spectroscopy (EDX, X-MaxN TSR) analyzer were to confirm the elemental composition of the electrode materials.

Electrochemical measurements: 80 wt% active materials (the as-prepared $BiPS_4$-based composite), 10 wt% super P as a conductive agent, and 10 wt% carboxymethylcelluloses (CMC) as a binder were dispersed in deionized water to form a homogeneous slurry. The slurry was then dried at 80 °C overnight under vacuum and punched into circular discs (d = 12 mm), and the loading of per disc was ~ 1.0 mg. CR2032 -type coin half cells were assembled in a glove box with Ar atmosphere (the content of H_2O and O_2 < 0.01 ppm), using glass fiber (GF/D, Whatman) as the separator and Na metal as a counter electrode. The electrolyte was prepared by uniform mixing 1 M $NaClO_4$ in propylene carbonate (PC) with a 5 wt% addition of fluoroethylene carbonate (FEC). Cyclic voltammetry (CV, CHI 660D, Shanghai) was tested between 0.01 to 3.0 V (versus Na/Na^+) at 0.1 mV s^{-1}. The galvanostatic charge/discharge curves were performed with a NEWARE battery test system in the voltage profile of 0.01-3.0 V (versus Na/Na^+) at room temperature. Electrochemical impedance spectroscopy (EIS, CHI 660D, Shanghai) measurements were conducted in the frequency range from 100 kHz to 0.01 Hz at 10 mV ac oscillation amplitude under open-circuit voltage status. In the full cell, the $Na_3V_2(PO_4)_3$ cathode and $BiPS_4$@MCNFs anode were paired up with an apporiate mass ratio. The electrochemical measurements is the same with the half cell.

DFT calculations: In order to investigate the effect of carbon materials on the diffusion of Na on $BiPS_4$, the DFT method were selected. For DFT method, all of the calculations were carried out using the Vienna Ab-initio Simulation Package (VASP). The projector augmented wave (PAW) method was used to describe the electrons-ionic interactions. The generalized gradient

approximation (GGA) together with the Perdew-Burke-Ernzerhof (PBE) was employed to describe all exchange and correlation effects. Moreover, the vdW interaction were also taken into account using DFT-D3 corrections. A 400 eV was chosen as the cutoff energy of the plane-wave basis to ensure the precision of calculations. Brillouin zone was sampled by a 2 × 2 × 1 k-point grid. The relaxation of the electronic degrees of freedom was assumed to be converged when the total energy changes between the two electronic optimization steps was smaller than 1×10^{-5} eV, and the forces below 0.03 eV/Å for ions were used as the criterion for relaxation convergence. We used climbing-image nudged elastic band (CI-NEB) method to calculate the diffusion barrier of Na on $BiPS_4$ and $BiPS_4$@MCNFs.

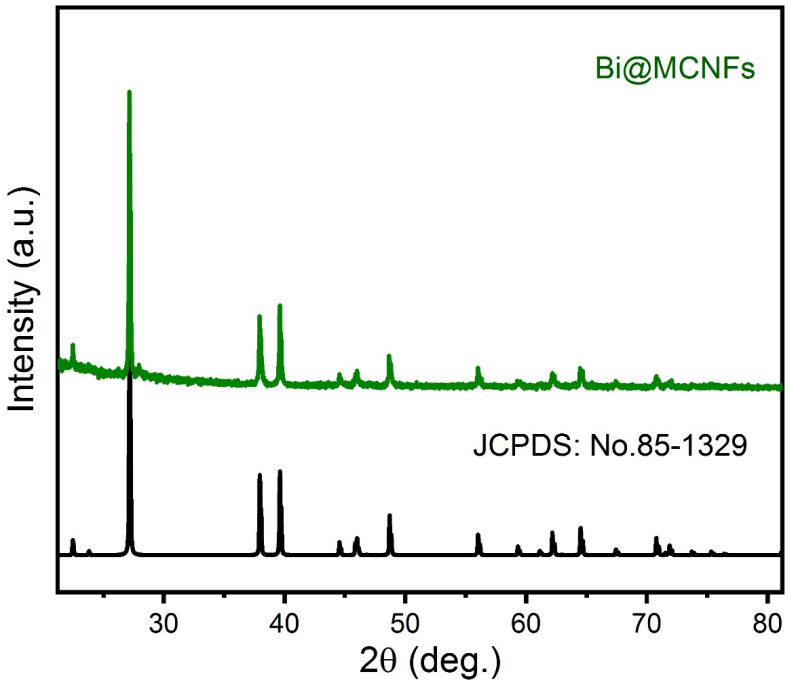

Figure S1. XRD pattern of the Bi@MCNFs. All the peak can be indexed to Bi (JCPDS card No. 85-1329) without any impurity peaks.

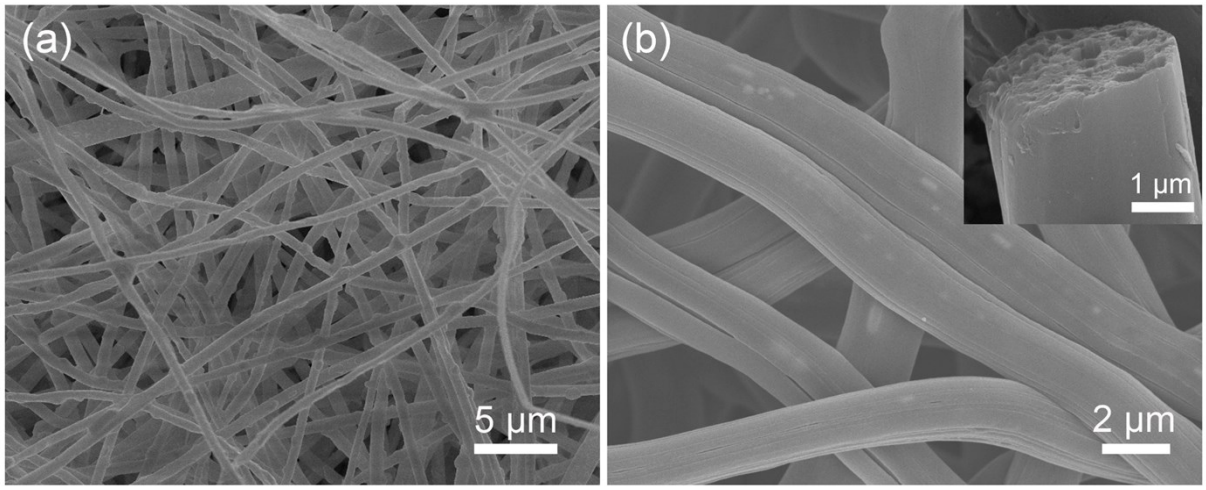

Figure S2. (a and b) SEM images of the Bi@MCNFs with different magnification. The inset in (b) shows the cross-section of the multichannel nanofibers.

Figure S2 shows the SEM images of the Bi@MCNFs with typical 1D multichannel fiberlike structures.

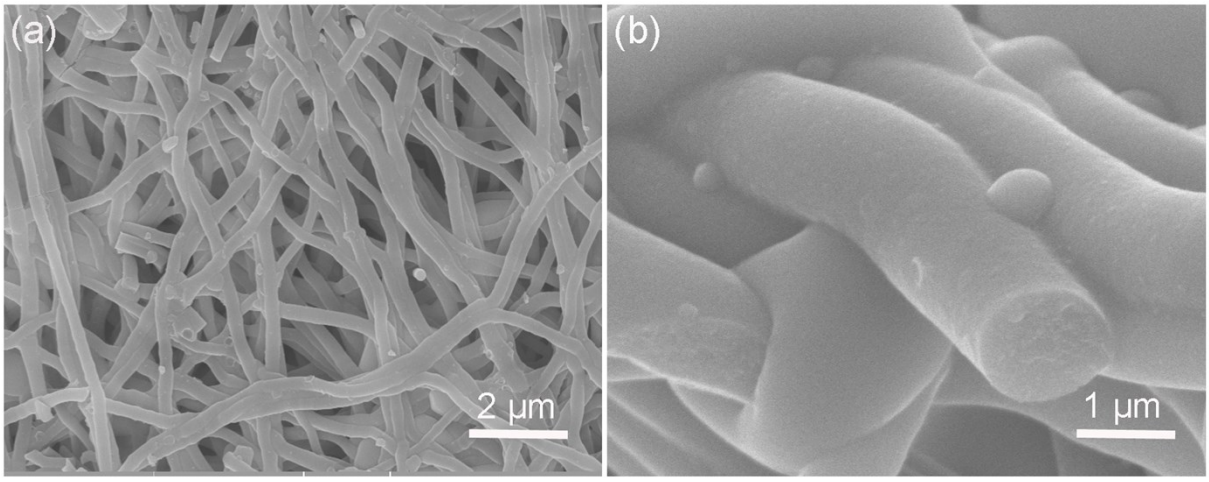

Figure S3. (a and b) SEM images of the $BiPS_4$@CNFs at different magnification.

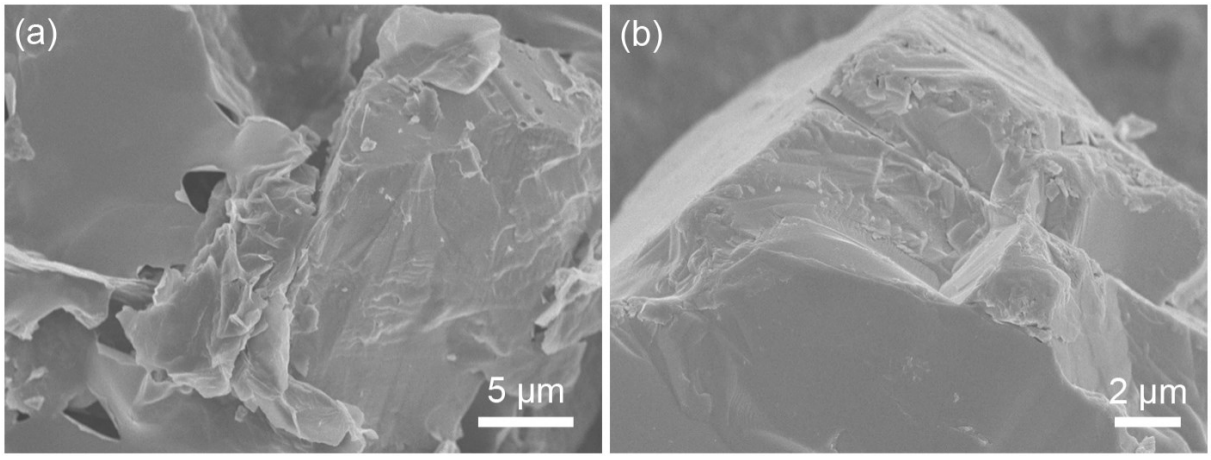

Figure S4. (a and b) SEM images of the $BiPS_4$ bulk at different magnification.

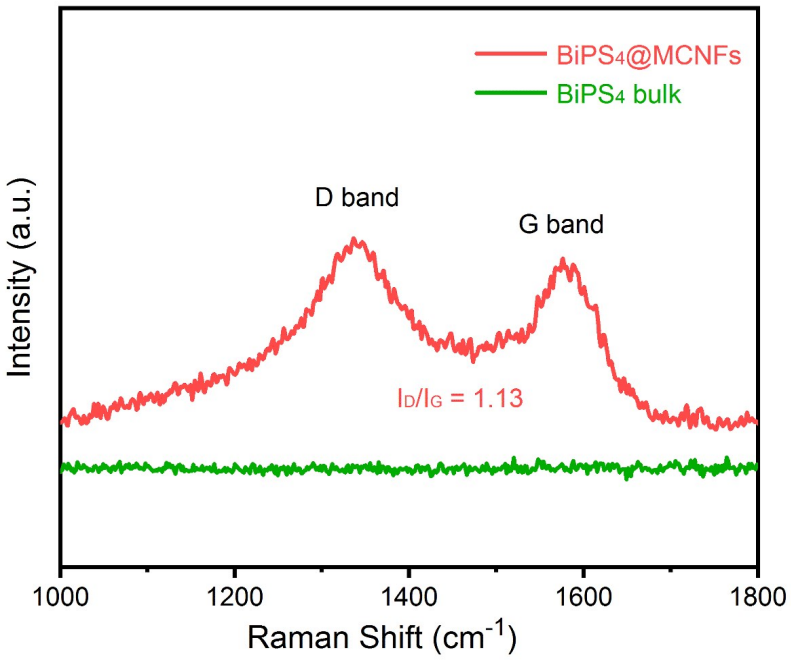

Figure S5. Raman Spectrum of $BiPS_4$ bulk and $BiPS_4$@MCNFs.

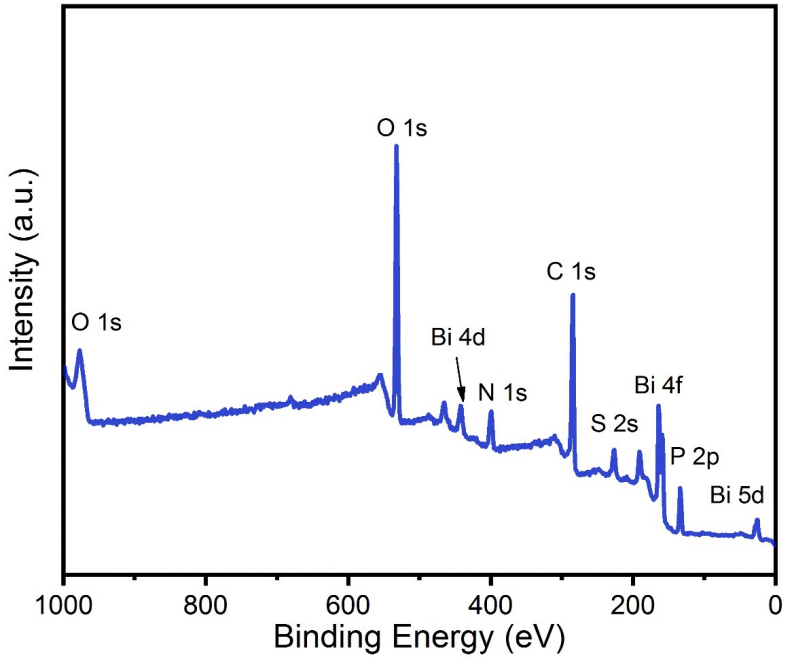

Figure S6. The XPS survey spectrum of $BiPS_4$@MCNFs.

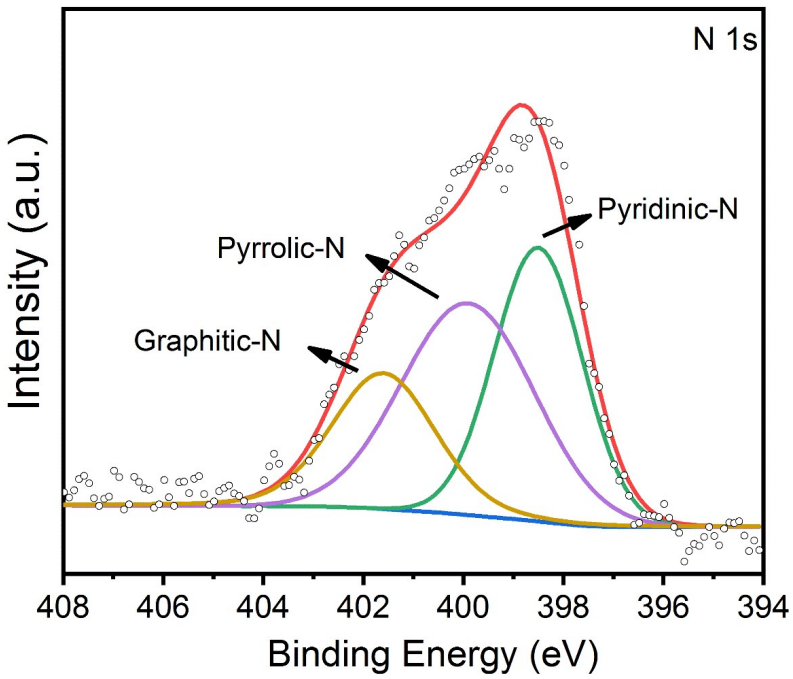

Figure S7. The N 1s XPS spectras of $BiPS_4$@MCNFs.

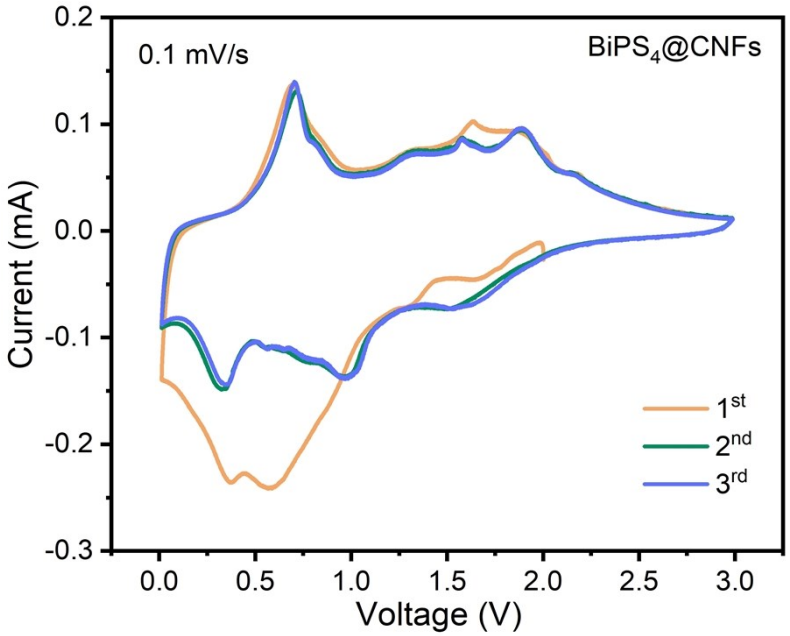

Figure S8. CV curves of $BiPS_4$@CNFs.

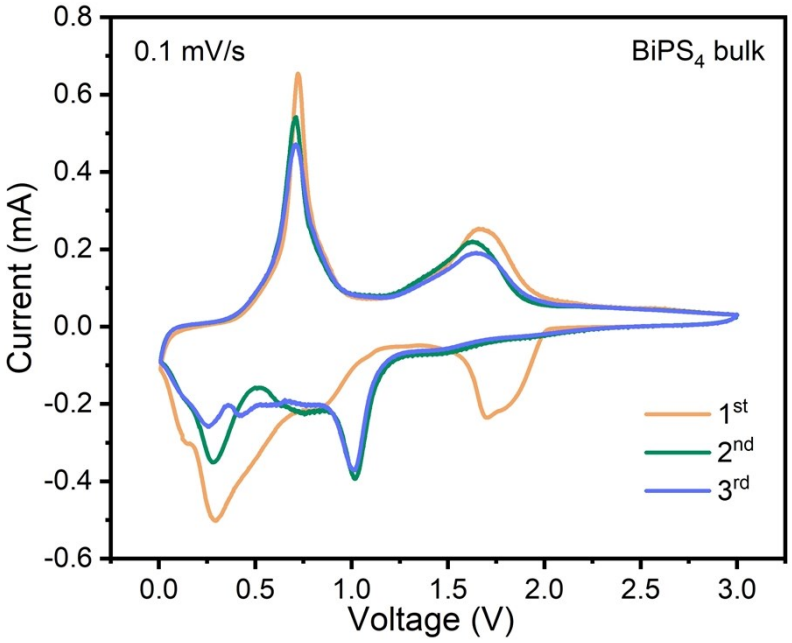

Figure S9. CV curves of $BiPS_4$ bulk.

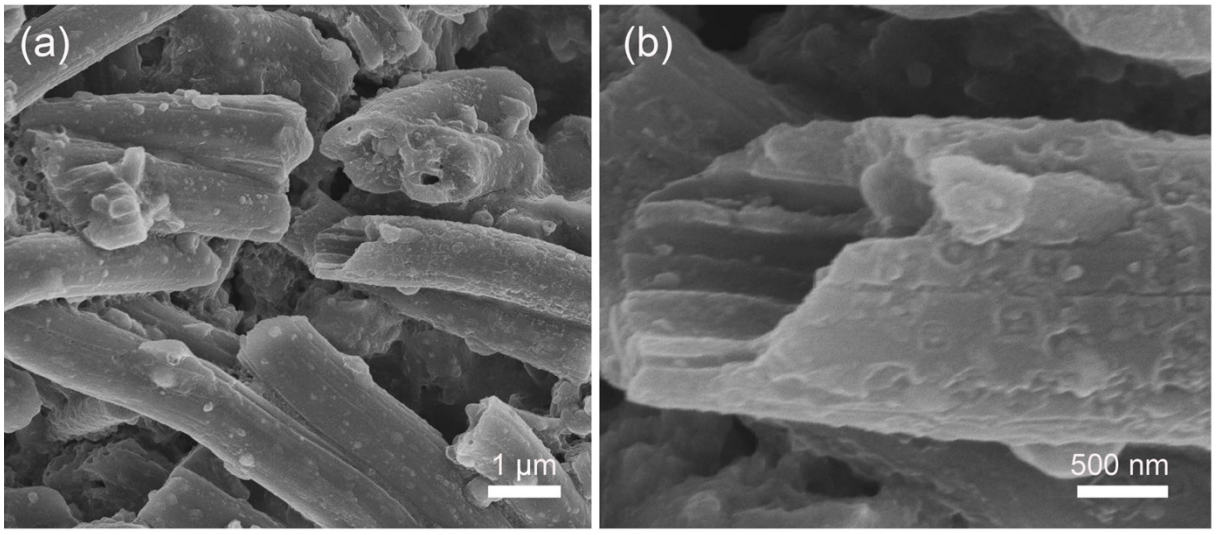

Figure S10. SEM images of the $BiPS_4$@ MCNFs electrode after 1000 cycles at 1 A g^{-1}.

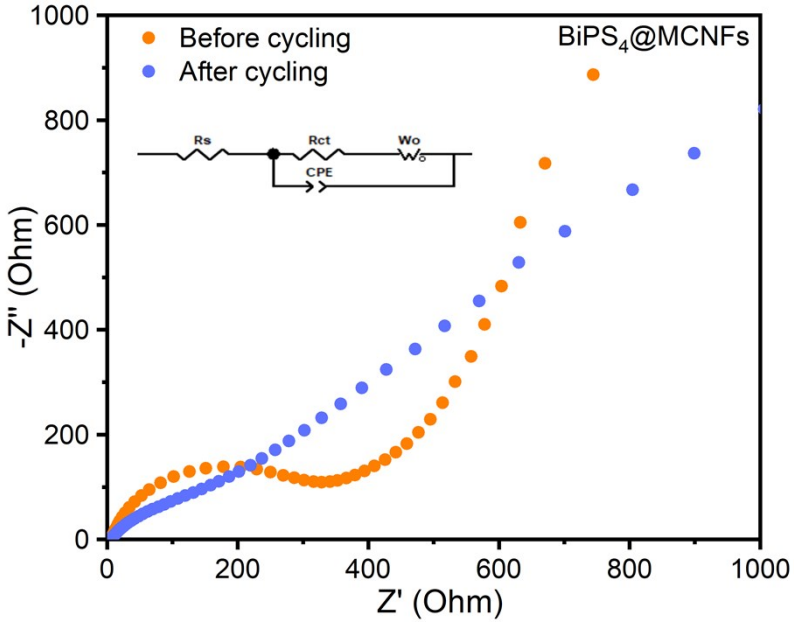

Figure S11. Nquist plots of $BiPS_4$@MCNFs before and after 10 cycles.

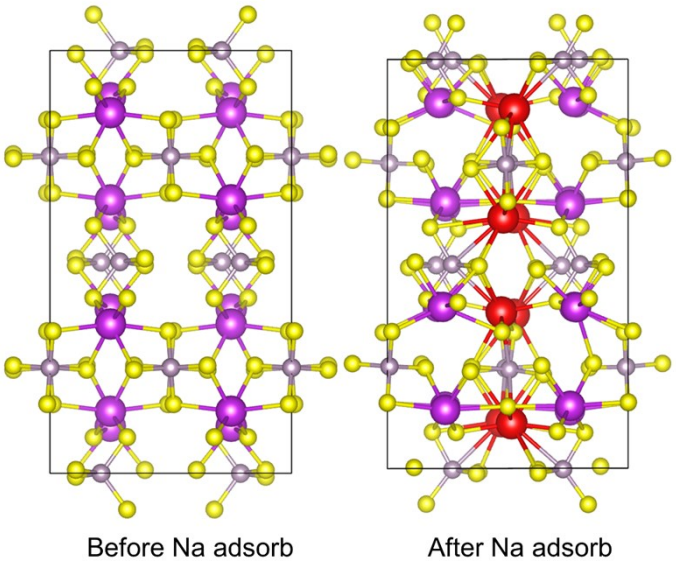

Figure S12. The structure of $BiPS_4$ and 8Na-$BiPS_4$.

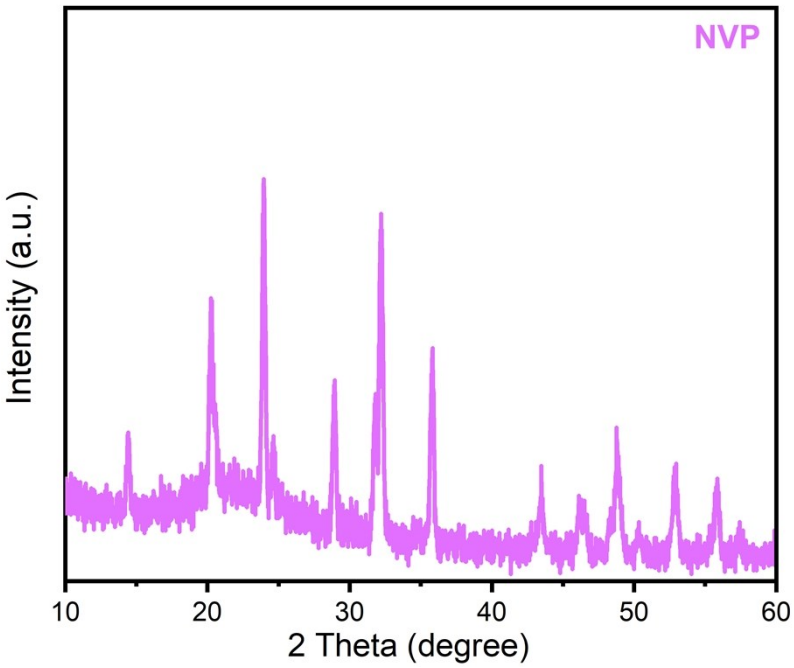

Figure S13. XRD pattern of $Na_3V_2(PO_4)_3$ (NVP) cathode.

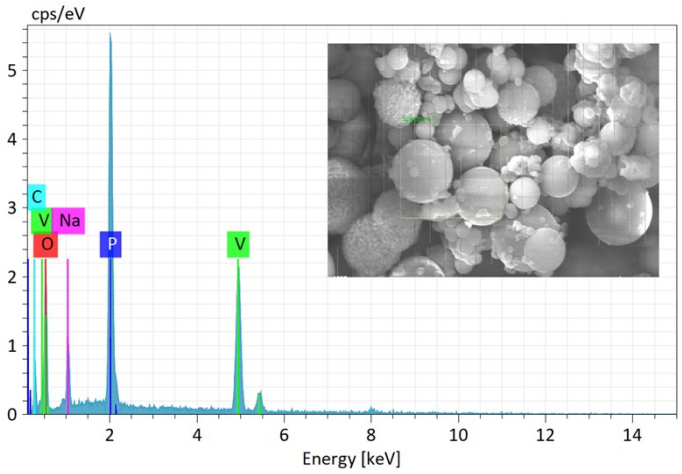

Figure S14. EDX results of the $Na_3V_2(PO_4)_3$ (NVP) cathode.

The NVP cathode is synthesized via ball-milling and then calcined the precursor in the argon atmosphere. The crystal structure of the as-obtained NVP cathode is characterized by XRD, which is finely matched with the monoclinic $Na_3V_2(PO_4)_3$ phase (JCPDS No.62-0345) (Figure S13 and S14).

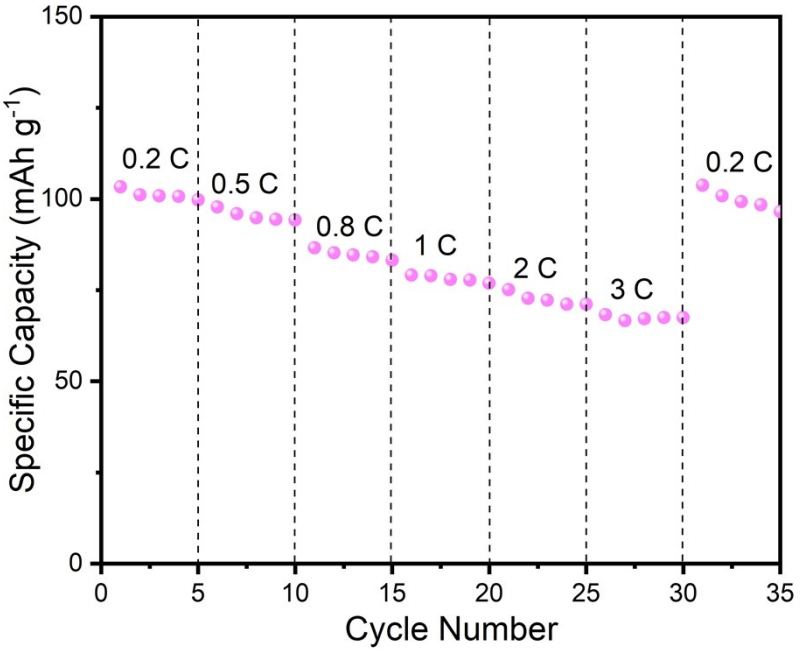

Figure S15. The rate performance of NVP cathode.

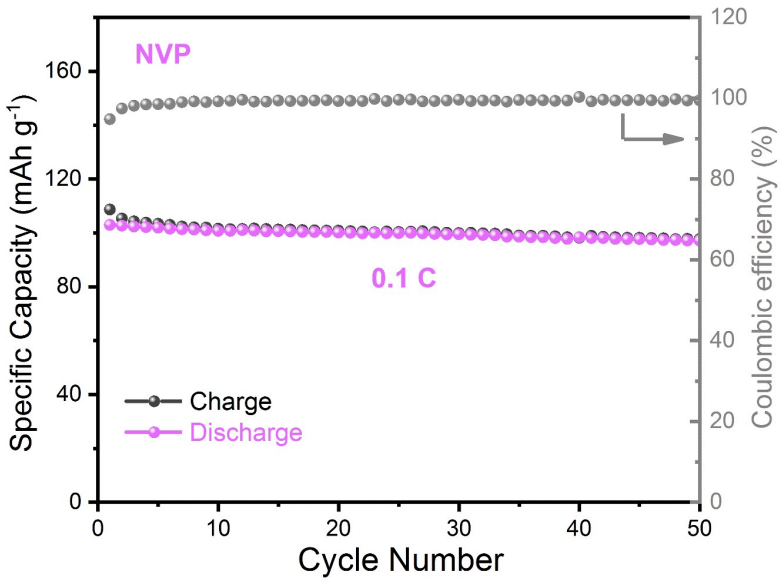

Figure S16. Cycling performance of NVP at 0.1 C.

The NVP cathode was tested in half cell using Na metal anodes. A stable cycling performance for 50 cycles and high rate capability were obtained for the NVP cathode, indicating that it is a reliable cathode material for SIBs, as shown in Figure S15 and S16.

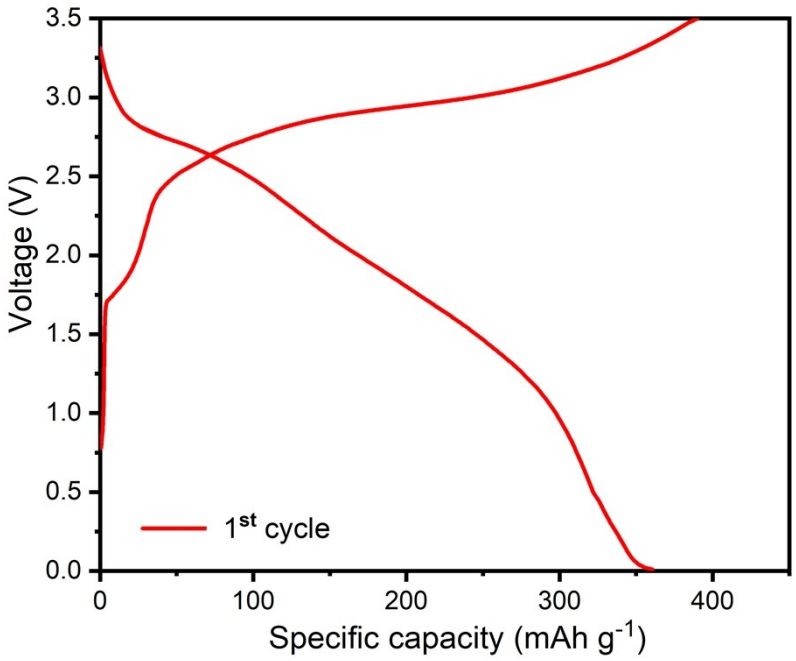

Figure S17. The initial charge/discharge curve of $BiPS_4$@MCNFs//NVP full cell at current density of 0.5 A g^{-1}.

Table S1. The fitted impedance data obtained from Nyquist plots using the circuit inset in Figure 3f.

Impedance Parameter	Electrode Materials		
	$BiPS_4$@MCNFs	$BiPS_4$@CNFs	$BiPS_4$ bulk
R_s/Ω	6.8	4.9	5.6
$R_{(ct)}/\Omega$	273	346	307

Table S2. Electrochemical performance of the recently reported transition metal-based anode materials for SIBs.

Materials	Current density ($A\ g^{-1}$)	Specific capacity ($mAh\ g^{-1}$)	Cycle number	Ref
Bi arrayed nanorods	0.05	350	150	[1]
Bi in carbon spheres	0.1	123.5	100	[2]
Bi@Graphite	20	150	10000	[3]
Bi@N-C	1.0	300	400	[4]
Bi nanoflakes	0.2	300	100	[5]
Bi/C	0.05	350	100	[6]
BiOCl/rGO	0.05	200	400	[7]
Bi_2S_3/GA	1.0	348	120	[8]
$Bi_{0.36}Sb_{0.64}$-C	0.1	370	50	[9]
$Bi_{0.94}Sb_{1.06}S_3$ nanorods	1.0	500	200	[10]
SnS_2@NPC	0.2	600	200	[11]
MoS_2@Graphene	0.02	600	100	[12]
Co_9S_8@Carbon	0.5	600	150	[13]
FeP@C@GR	0.1	400	250	[14]
$FePS_3$@Mxene	0.5	527	90	[15]
$Sn_2P_2S_6$	1.0	500	500	[16]
$BiPS_4$@MCNFs	1.0	410	1000	This work

Table S3. The lattice parameters of $BiPS_4$ before and after 8Na adsorption.

	a (Å)	b (Å)	c (Å)	α (°)	β (°)	γ (°)
Before	10.58	11.17	19.57	90.0	90.0	90.0
After	11.25	11.47	19.50	89.9	89.9	90.0
Δ	0.67	0.30	0.07	0.1	0.1	0.0

Reference

[1] S. Liu, J. Feng, X. Bian, J. Liu, H. Xu, *J. Mater. Chem. A* **2016**, *4*, 10098.

[2] W. Zuo, W. Zhu, D. Zhao, Y. Sun, Y. Li, J. Liu, X. W. Lou, *Energy Environ. Sci.* **2016**, *9*, 2881.

[3] J. Chen, X. Fan, X. Ji, T. Gao, S. Hou, X. Zhou, L. Wang, F. Wang, C. Yang, L. Chen, C. Wang, *Energy Environ. Sci.* **2018**, *11*, 1218.

[4] H. Yang, R. Xu, Y. Yao, S. Ye, X. Zhou, Y. Yu, *Adv. Funct. Mater.* **2019**, *29*, 1809195.

[5] L. Wang, C. Wang, F. Li, F. Cheng, J. Chen, *Chem. Commun.* **2017**, *54*, 38.

[6] J. Sottmann, M. Herrmann, P. Vajeeston, Y. Hu, A. Ruud, C. Drathen, H. Emerich, H. Fjellvag, D. S. Wragg, *Chem. Mater.* **2016**, *28*, 2750.

[7] J. Sun, W. Tu, C. Chen, A. Plewa, H. Ye, J. A. S. Oh, L. He, T. Wu, K. Zeng, L. Lu, *Chem. Mater.* **2019**, *31*, 7311.

[8] Y. Zhang, L. Fan, P. Wang, Y. Yin, X. Zhang, N. Zhang, K. Sun, *Nanoscale* **2017**, *9*, 17694.

[9] Y. Zhao, A. Manthiram, *Chem. Mater.* **2015**, *27*, 3096.

[10] J. Ni, X. Bi, Y. Jiang, L. Li, J. Lu, *Nano Energy* **2017**, *34*, 356.

[11] X. Xu, R. Zhao, B. Chen, L. Wu, C. Zou, W. Ai, H. Zhang, W. Huang, T. Yu, *Adv. Mater.* **2019**, *31*, 1900526.

[12] X. Xie, Z. Ao, D. Su, J. Zhang, G. Wang, *Adv. Funct. Mater.* **2015**, *25*, 1393.

[13] X. Li, K. Li, S. Zhu, K. Fan, L. Lyu, H. Yao, Y. Li, J. Hu, H. Huang, Y. W. Mai, J. B. Goodenough, *Angew. Chem. Int. Ed.* **2019**, *58*, 6239.

[14] X. Wang, K. Chen, G. Wang, X. Liu, H. Wang, *ACS Nano* **2017**, *11*, 11602.

[15] Y. Ding, Y. Chen, N. Xu, X. Lian, L. Li, Y. Hu, S. Peng, *Nano-Micro Lett.* **2020**, *12*, 54.

[16] S. Huang, C. Meng, M. Xiao, S. Ren, S. Wang, D. Han, Y. Li, Y. Meng, *Small* **2018**, *14*, 1704367.